LAWRENCE
LIVERMORE
NATIONAL
LABORATORY

LLNL-JRNL-666571

Lasers, Extreme UV and Soft X-ray

J. Nilsen

January 27, 2015

The Optics Encyclopedia

Disclaimer

Lasers, Extreme UV and Soft X-ray

Joseph Nilsen

Lawrence Livermore National Laboratory, Livermore, CA 94551-0808
(925) 422-4766 JNILSEN@LLNL.GOV

Abstract
Three decades ago, large ICF lasers that occupied entire buildings were used as the energy sources to drive the first X-ray lasers. Today X-ray lasers are tabletop, spatially coherent, high-repetition rate lasers that enable many of the standard optical techniques such as interferometry to be extended to the soft X-ray regime between wavelengths of 10 and 50 nm. Over the last decade X-ray laser performance has been improved by the use of the grazing incidence geometry, diode-pumped solid-state lasers, and seeding techniques. The dominant X-ray laser schemes are the monopole collisional excitation lasers either driven by chirped pulse amplification (CPA) laser systems or capillary discharge. The CPA systems drive lasing in neon-like or nickel-like ions, typically in the 10 – 30 nm range, while the capillary system works best for neon-like argon at 46.9 nm. Most researchers use nickel-like ion lasers near 14 nm because they are well matched to the Mo:Si multilayer mirrors that have peak reflectivity near 13 nm and are used in many applications. The last decade has seen the birth of the X-ray free electron laser (XFEL) that can reach wavelengths down to 0.15 nm and the inner-shell Ne laser at 1.46 nm.

Keywords: Neon-like, Nickel-like, collisional excitation, X-ray free electron laser

1 Introduction

Since the original article (oe037) was published a decade ago most of the X-ray laser research has focused on using the X-ray laser as a diagnostic tool for studying materials using traditional laser techniques such as interferometry but at the shorter wavelength of the X-ray laser. Most of this research utilizes the well-developed nickel-like collisional excitation lasers that lase near 14 nm (i.e. Pd at 14.7 nm, Ag at 13.9 nm) since these are well matched to the Mo:Si multilayer mirrors that have high reflectivity at normal incidence. The nickel-like ions lase on the 4d $^1S_0 \rightarrow$ 4p $^1P_1$ transition. The 4d $^1S_0$ upper laser level is populated by the monopole collisional excitation from the nickel-like ground state that consists of 28 electrons filling the closed K, L, and M-shells. The analogous scheme in neon-like ions lases on the 3p $^1S_0 \rightarrow$ 3s $^1P_1$ transition.

A good source of information on this research are the conference proceedings from the biennial International Conference on X-ray lasers listed at the end of the references.

Recall that the typical nickel-like laser is created by illuminating a solid target with a line-focused optical laser that has a nanosecond prepulse to create the plasma and a picosecond laser pulse to heat the plasma to lasing conditions. The use of the prepulse technique [1] together with availability of short pulse lasers with pulse lengths less than a psec were the enabling technologies for tabletop X-ray lasers. The X-ray laser uses amplified spontaneous emission (ASE) without a laser cavity so the spatial coherence is limited and the divergence depends on the aspect ratio of the line focus and the subsequent plasma column that is created. Since laser applications require lasers with good output characteristics most of the X-ray laser development has been focused on improving the spatial coherence of the X-ray laser, reducing the optical laser drive requirements, and increasing the repetition rate. In this article we will describe how the use of the grazing incidence geometry has reduced the laser drive requirements to less than one joule per pulse and thereby increased the repetition rate. The use of very coherent high harmonic radiation to seed the X-ray lasers has greatly increased the spatial coherence of the X-ray laser output.

In terms of new X-ray laser developments the big breakthrough has been the emergence of the X-ray free electron laser (XFEL) over the last decade. While the XFEL currently requires a large accelerator facility such as the two-mile long linear accelerator at Stanford it can reach wavelengths as short as 0.15 nm. There is a separate article on free electron lasers (see oe038 and oe038.pub2) but this article includes a brief summary of the XFEL output characteristics. One new X-ray laser that has emerged that uses the XFEL as a drive laser is the inner-shell Ne laser at 1.46 nm. This is discussed in some detail.

2 Improving Tabletop Laser-Driven X-ray Lasers

A decade ago the newest variant of the prepulse technique used a combination of a nsec laser prepulse to illuminate a solid target to create the plasma and a psec laser pulse to heat the plasma to lasing conditions. That is still the primary method used today and enabled the use of much smaller lasers to drive the neon-like and nickel-like X-ray lasers. Those lasers use chirped pulse amplification (CPA) [2,3] to produce the psec duration drive pulse with typical energies less than 10 J. The nsec prepulse is created by using part of the uncompressed beam from the CPA system. Typical experiments used less than 10 J in each beam. These systems are compact, tabletop, higher-repetition rate systems that occupy a few standard optical benches and have largely replaced the building size, inertial confinement fusion (ICF) lasers used in the past. Given the short pulse duration these experiments use a travelling wave geometry to transversely illuminate the X-ray laser target and synchronize the pumping with the lasing process at the speed of light. This causes the X-ray lasing to preferentially emit from one end of the laser. The big change in the last decade is using a grazing incidence geometry to illuminate the target and reduce the drive requirements by an order of magnitude and the use of high harmonics to seed the X-ray laser and create a more spatially coherent output.

2.1 Grazing incidence geometry

The tabletop X-ray lasers of a decade ago used a line-focused CPA laser that illuminated the target at normal incidence with a prepulse followed by a short main pulse. For an example see Fig. 1 in oe037. This geometry wastes a lot of the drive energy because the optical laser energy is mainly absorbed at the critical density for the optical light, which is an electron density of 1.7 x 10^{21} cm^{-3} for a 0.8 μm Ti:sapphire laser drive, while the gain region for the X-ray laser typically has an electron density significantly below critical density. To improve the efficiency it was demonstrated that illuminating the target with the optical laser at a grazing angle would better couple the optical laser energy into the region of the plasma with X-ray laser gain. This pumping geometry improves the laser coupling efficiency into the gain region of the plasma by using refraction to turn the pump laser at an electron density below the critical density, thus increasing the path length and absorption in this specific region of the plasma. This was first demonstrated with a nickel-like molybdenum target that lases at 18.9 nm on the 4d $^1S_0 \rightarrow$ 4p $^1P_1$ transition [4]. For that case the optimum lasing was predicted to be at an electron density of 10^{20} cm^{-3}. The optimum grazing angle ϕ can be estimated from n_e(gain region) = n_e(critical) $\sin^2(\phi)$ which gives $\phi = 14°$ for this case. With this shallow angle, as shown in Fig. 1, one achieves a travelling wave velocity of $c/\cos(\phi) = 1.03$ c, where c is the speed of light [5]. It was shown that by tilting the compression grating for the CPA system one could achieve a travelling wave velocity of 1.0 c. [5,6]. The higher efficiency of the grazing incidence pumping geometry, commonly known as the GRIP geometry, requires only a very low energy laser pump (<150 mJ), available at a 10 Hz repetition rate and represents more than an order of magnitude reduction in the pumping energy compared to the conventional transverse scheme.

Improvements in optical lasers has led to the replacement of flash lamps with diodes to create diode-pumped solid state lasers such as Yb:YAG amplifiers that produce up to 1J of output at 100 Hz. [7]. Utilizing a 1.03 μm Yb:YAG laser with 0.9 J of output at 100 Hz in the GRIP geometry to drive a silver target enabled the production of a saturated nickel-like silver X-ray laser that produces 1.0 μJ of output at 13.9 nm from a 0.5 cm long target [8]. Other nickel-like lasers ranging from Pd (Z=46) to Te (Z=52) have been produced with this system. Similar results are being achieved in many laboratories with wavelengths as short as 6.85 nm in nickel-like samarium using a 10 J drive in the GRIP geometry [9].

2.2 Seeding of X-ray laser by high harmonics

Most X-ray lasers have no laser cavities so the laser output is seeded by spontaneous emission and the total output is just the amplified spontaneous emission (ASE) with the divergence and spatial coherence determined by the aspect ratio of the plasma column. The temporal coherence is determined by the line width of the atomic transition, which tends to be quite narrow and have a bandwidth, $\Delta\lambda/\lambda < 10^{-4}$.

To improve the spatial coherence of the X-ray laser many researchers are trying to seed the X-ray laser with high-harmonic radiation that has the high spatial coherence intrinsic to the optical drive laser. An early attempt used the 25th harmonic of the Ti:sapphire laser to seed the nickel-like krypton laser at 32.8 nm and observed promising improvements in the spatial coherence [10].

A more recent example of seeding is the use of the 59th harmonic of the 780 nm Ti:sapphire laser to seed the nickel-like cadmium laser at 13.2 nm [11]. The 59th harmonic is created by focusing 20mJ of the Ti:sapphire laser into a Ne gas jet. The high harmonic was imaged onto the input of the X-ray laser. The 0.35-cm long Ni-like Cd X-ray laser target was driven by a 6.8 psec, 350 mJ prepulse and the 50 fsec, 0.85 J main pulse from the Ti:sapphire laser incident at a grazing incidence angle of 23°. One of the main challenges of using high harmonics to seed X-ray lasers is the much larger linewidth of the high harmonics which means most of the energy in the high harmonic is not amplified. In this case the linewidth of the high harmonic was ≅ 0.03 nm compared with 0.01 nm for the X-ray laser. For this Ni-like Cd laser the output was less than 1% fully spatially coherent without the seeding while the coherence length increases dramatically to 70 μm for an X-ray laser with a beam diameter of 80-90 μm at a distance of 10 cm from the exit of the amplifier. Understanding how to seed the X-ray laser and improve its spatial coherence is an area of ongoing research that shows great promise.

3 Alternative X-ray laser schemes

3.1 X-ray Free Electron Laser

A decade ago the best candidate for a new X-ray laser scheme was the extension of the free electron laser technology into the X-ray regime. At that time experiments had observed lasing at 100 nm using the TESLA Test Facility at the Deutsches Elektronen-Synchrotron (DESY) in Hamburg [12]. That and other proposed facilities used self-amplified spontaneous emission (SASE) to obtain high gain in a single pass. While this scheme does not lase on an atomic transition like traditional lasers it does produce coherent X-ray output.

Over the last decade the X-ray free electron laser (XFEL) has become reality. FLASH [13-15] is a small version of the European XFEL at DESY that was commissioned in 2004 and has been used for research since 2005. The facility is 260 meters long and generates soft X-ray radiation in the wavelength range from 4.2 – 45 nm in the first harmonic with GW peak power and pulse durations from 50 - 200 fsec.

The European XFEL [15] will run from the DESY site in Hamburg to the research site in Schenefeld (Schleswig-Holstein). It will start user operation in 2017 and expects to achieve peak brilliance of 5 x 10^{33} photons/sec/mm^2/mrad^2/0.1% bandwidth with pulse duration less than 100 fsec and wavelength between 0.05 to 6 nm.

The largest XFEL facility currently operating is at the two-mile-long linear accelerator at Stanford [16,17]. The Linac Coherent Light Source (LCLS) was constructed using the last one-third of the original linear accelerator and achieved X-ray lasing in April 2009. It can produce X-rays down to 0.1 nm with peak brilliance of 10^{33} photons/sec/mm^2/mrad^2/0.1% bandwidth, pulse duration of 2 - 300 fsec, at a 120 Hz repetition rate.

FERMI@Elettra is a single-pass FEL user-facility covering the wavelength range from 100 nm to 10 nm, located next to the third-generation synchrotron radiation facility ELETTRA in Trieste, Italy [18].

The Spring-8 Angstrom Compact Free Electron Laser (SACLA) is the most compact XFEL in the world and can operate at wavelengths as short as 0.06 nm [19-21]. SACLA was completed in 2011 and is 700 meters long as compared with the 3 km length of LCLS.

XFEL's are being constructed at many sites around the world that currently have accelerators. The Swiss XFEL [22] at the Paul Scherrer Institut is expected to come online in 2016 and reach wavelengths as short as 0.1 nm. The XFEL at the Pohang Accelerator Laboratory in Korea [23] is expected to be completed in 2015 and also reach wavelengths as short as 0.1 nm.

A more detailed description of free electron lasers can be found in another chapter of this publication. See oe038 and the update oe038.pub2.

3.2 Inner-shell excitation

To reach shorter wavelength more efficiently researchers have suggested lasing on inner shell transitions, such as the Kα line [24], in materials such as singly-ionized carbon [25]. The idea, suggested in the 1970's, is to use a short pulse of X-rays to selectively ionize the 1s electron and lase on the 2p → 1s transition before autoionization destroys the inversion [26]. Since the autoionization rates are typically 10^{14} sec^{-1} it requires an X-ray pulse with a duration of fsecs. While fsec optical lasers have been available for many years it has been difficult to convert the optical light into a short bright X-ray pulse. That problem has been solved using the XFEL as the very bright X-ray source to photo-ionize the 1s electron.

In 2011 the dream of demonstrating an inner-shell X-ray laser was realized at the SLAC Linac Coherent Light Source when the X-ray free electron laser at 1.29 nm was used to photo-ionize the K-shell of neutral neon gas and create lasing on the 2p → 1s transition at 1.46 nm in singly ionized neon gas, as shown in Fig. 2. [27]. The natural lifetime of the laser transition is 135 fsec. The challenge with achieving lasing is that the autoionization lifetime of the upper laser state is 2.3 fsec. The XFEL beam is sufficiently bright that the photo-ionization rate for the 1s electron is comparable to the autoionization (Auger) rate. For these experiments an effective gain of 61-70 cm^{-1} was estimated using a 0.28-cm long target.

3.3 Resonant photopumping schemes

The idea to create an inversion by using radiation from a bright line in one ion to pump a resonant transition in another ion and populate an excited state that could lase has been investigated for many decades. A classic scheme proposed in the 70's was to use the He-α line of Na to resonantly photo-pump the He-γ line of Ne. Lasing would then be expected on several 4f → 3d lines in helium-like neon at wavelengths near 23 nm [28]. Many experiments were tried using pulsed power machines but gain and lasing have never been observed even though measurements of the line emission suggests that gain does exist in the plasma [29-31]. Many photopumped schemes have been suggested and

even tested experimentally but the results have been disappointing. The biggest challenge that needed to be overcome is finding an adequate resonance between a strong pump line and a potential lasing material.

The only successful photopumped X-ray laser schemes have been the self-photopumped schemes that use radiation trapping of a strong resonance lines to drive lasing in materials such as neon-like argon [32,33] and titanium [34] at 45 nm and 30.1 nm, respectively, and nickel-like molybdenum [35] at 22.6 nm.

That should all change in the future with the XFEL as the source of a strong monochromatic X-ray pump that can be tuned to the atomic resonances. One current limitation is that most XFEL's have a large bandwidth (as much as 1% of the photon energy) but it is hoped that by seeding the XFEL the bandwidth of the X-ray emission can be significantly reduced [15,17,21].

4 Conclusion

Tremendous progress has been made over the last decade to produce tabletop, spatially coherent, high-repetition rate X-ray lasers that enable many of the standard optical techniques such as interferometry to be extended to the soft X-ray regime between wavelengths of 10 and 50 nm. X-ray laser performance has been improved by the use of the grazing incidence geometry, diode-pumped solid-state lasers, and seeding techniques. The dominant X-ray laser schemes are the monopole collisional excitation lasers either driven by chirped pulse amplification (CPA) laser systems or capillary discharge. The CPA systems drive lasing in neon-like or nickel-like ions, typically in the 10 – 30 nm range, while the capillary system works best for neon-like argon at 46.9 nm. Most researchers use nickel-like ion lasers near 14 nm because they are well matched to the Mo:Si multilayer mirrors that have peak reflectivity near 13 nm and are used in many applications. The last decade has seen the birth of the X-ray free electron laser (XFEL) that can reach wavelengths down to 0.15 nm and the inner-shell Ne laser at 1.46 nm. The availability of the XFEL as a very bright X-ray line source opens up the possibility of driving many new types of photopumped X-ray laser schemes.

Table 1 from oe037 gives a short list of some of the X-ray lasers being used today. An extensive list of X-ray laser wavelengths can be found in the handbook by Weber and Refs. 36-38.

The efficiency of pumping X-ray lasers is still very low, typically 10^{-6}. The low efficiency offers the potential for tremendous improvement in the future.

Acknowledgement

This work was performed under the auspices of the U.S. Department of Energy by Lawrence Livermore National Laboratory under Contract DE-AC52-07NA27344.

Glossary

Neon-like: An ionic stage where an atom has been ionized such that there are 10 bound electrons. The energy level structure is very similar to that of neutral neon and the ground state has filled K and L shells.

Nickel-like: An ionic stage where an atom has been ionized such that there are 28 bound electrons. The ground state has filled K, L, and M shells.

ICF: Inertial confinement fusion. The largest optical lasers such as Nova and NIF at LLNL were built to demonstrate ICF.

Collisional excitation: Process by which free electrons in the plasma excite bound electrons to a higher energy bound state by transferring part of their energy.

Metastable: An excited bound state in the ion that can not decay to another bound state with different principal quantum number by direct dipole allowed radiative transition.

Travelling wave geometry: A situation by which the optical laser illuminates the target synchronously with the x-rays travelling in the amplification direction. For transverse illumination this is typically done by changing the phase front of the optical laser using a grating or stepped mirror.

Gain-length product: The integral of the gain over the length of the gain medium including the effect of saturation on the gain. Typically gain-length products of about 15 are needed for the x-ray laser to reach saturation intensity.

Saturation intensity: The x-ray laser intensity at which the gain is reduced by a factor of two due to stimulated emission in the plasma modifying the populations of the laser states.

Radiation trapping: A process by which the radiation emission from a strong resonance line builds up sufficient intensity that the population of the lower laser state increases and starts to quench the gain of the x-ray laser transition.

References

[1] Nilsen, J., MacGowan, B. J., Da Silva, L. B., Moreno, J. C. (1993), Phys. Rev. A **48**, 4682 - 4685.

[2] Kalachnikov, M., Nickles, P. V., Schnürer, M., Will, I., Sandner, W. (1997), Opt. Comm. **133**, 216 – 220.

[3] Sullivan, A., Bonlie, J., Price, D. F., White, W. E. (1996), Opt. Lett. **21**, 603 – 605.

[4] Keenan, R., Dunn, J., Patel, P. K., Price, D. F., Smith, R. F., Shlyaptsev, V. N. (2005), Phys. Rev. Lett. **94**, 103901.

[5] Bleiner, D., Feurer, T. (2014), *Springer Proceedings in Physics Volume 147 - X-ray Lasers 2012,* S. Sebban, J. Gautier, D. Ros, and P. Zeitoun, eds., (Springer, Dordrecht, The Netherlands, 2014) pp. 35-38.

[6] Chanteloup, J-C, Salmon, E., Sauteret, C., Migus, A., Zeitoun, Ph., Klisnick, A., Carillon, A., Hubert, S. Ros, D., Nickles, P., Kalachnikov, M. (2000), J. Opt. Soc. Am. B **17**, 151-157.

[7] Curtis, A. H., Reagan, B. A., Wernsing, K. A., Furch, F. J. Luther, B. M., Rocca, J. J. (2011), Opt. Lett. **36**, 2164-2166.

[8] Reagan, B. A., Berrill, M., Wernsing, K. A., Baumgarten, C., Woolston, M., Rocca, J. J. (2014), Phys. Rev. A **89**, 053820.

[9] Balmer, J., Staub, F., Jia, F., (2014), *Springer Proceedings in Physics Volume 147 - X-ray Lasers 2012,* S. Sebban, J. Gautier, D. Ros, and P. Zeitoun, eds., (Springer, Dordrecht, The Netherlands, 2014) pp. 29-34.

[10] Zeitoun, Ph., Faivre, G., Sebban, S., Mocek, T. , Hallou, A. , Fajardo, M. , Aubert, D., Balcou, Ph., Burgy, F., Douillet, D., Kazamias, S., de Lache`ze-Murel, G., Lefrou, T., le Pape, S., Merce`re, P., Merdji, H., Morlens, A. S., Rousseau, J. P., Valentin, C. (2004), Nature **431**, 426-429.

[11] Pedaci, F., Wang, Y., Berrill, M., Luther, B., Granados, E., Rocca, J. J. (2008), Opt. Lett. **33**, 491-493.

[12] Feldhaus, J. (2001), J.Phys. IV(France) **11**, (Pr2) 237-244.

[13] Tiedtke, K., Azima, A. et al. (2009), New. J. Phys. **11**, 023029.

[14] Feldhaus, J. (2010), J. Phys. B. **43**, 194002. [FLASH]

[15] Feldhaus, J., Krikunova, M., Meyer, M., Möller, Th., Moshammer, R., Rudenko, A., Tschentscher, Th., Ullrich, J. (2013), J. Phys. B. **46**, 164002.

[16] Emma, P. et al. (2010), Nature Photonics **4**, 641-647.

[17] Bostedt, C. et al. (2013), J. Phys. B **46**, 164003.

[18] Bocchetta, C. J. et al. (2003), Nucl. Inst. And Meth. A **507**, 484 – 488.

[19] Huang, Z., Lindau, I. (2012), Nature Photonics **6**, 505-506.

[20] Tanaka, H., Yabashi, M. et al. (2012), Nature Photonics **6**, 540-544.

[21] Yabashi, M., Tanaka, H. et al. (2013), J. Phys. B. **46**, 164001.

[22] Information on Swiss XFEL is available at http://www.psi.ch/media/overview-swissfel

[23] Information on Korean XFEL at Pohang is available at http://pal.postech.ac.kr/paleng

[24] Elton, R. C. (1975), Appl. Opt. **14**, 2243 - 2249.

[25] Moon, S. J., Eder, D. C. (1998), Phys. Rev. A. **57**, 1391 - 1394.

[26] Axelrod, T. S. (1976), Phys. Rev. A **13**, 376 – 382.

[27] Rohringer, N., Ryan, D., London, R. A., Purvis, M., Albert, F., Dunn, J., Bozek, J. D., Bostedt, C., Graf, A., Hill, R., Hau-Riege, S. P., Rocca, J. J. (2012), Nature **481**, 488-491.

[28] Nilsen, J., Scofield, J. H., Chandler, E. A. (1992), Appl. Opt. **31**, 4950.

[29] Porter, J. L., Spielman, R. B., Matzen, M. K., McGuire, E. J., Ruggles, L. E., Vargas, M. F., Apruzese, J. P., Clark, R. W., Davis, J. (1992), Phys. Rev. Lett. **68**, 796–799.

[30] Apruzese, J. P., Davis, J. (1985), Phys. Rev. A **31**, 2976 – 2983.

[31] Nilsen, J., Chandler, E. (1991), Phys. Rev. A **44**, 4591 – 4598.

[32] Nilsen, J., Fiedorowicz, H., Bartnik, A., Li, Y. L., Lu, P. X., Fill, E. E. (1996), Opt. Lett. **26**, 1403 – 1405.

[33] Fiedorowicz, H., Bartnik, A., Dunn, J., Smith, R. F., Hunter, J., Nilsen, J., Osterheld, A. L., Shlyaptsev, V. N. (2001), Opt. Lett. **26**, 1403 – 1405.

[34] Kalachnikov, M. P., Nickles, P. V., Schnürer, M., Sandner, W., Shlyaptsev, V. N., Danson, C., Neely, D., Wolfrum, E., Zhang, J., Behjat, A., Demir, A., Tallents, G. J., Warwick, P. J., Lewis, C. L. S. (1998), Phys. Rev. A **57**, 4778–4783.

[35] Nilsen, J., Dunn, J., Osterheld, A. L., Li, Y. L. (1999), Phys. Rev. A **60**, R2677 – 2680.

[36] Nilsen, J., Scofield, J. H. (1994), Physica Scripta **49**, 588 – 591.

[37] Li, Y. L., Nilsen, J., Dunn, J., Osterheld, A. L., Ryabtsev, A., Churilov, S. (1998), Phys. Rev. A **58**, R2668 - 2671.

[38] Nilsen, J., Dunn, J., Osterheld, A. L., Li, Y. L. (1999), Phys. Rev. A **60**, R2677 – 2680.

Further Reading

R. C. Elton (1990), *X-ray Lasers*, San Diego, CA: Academic Press

M. J. Weber (Ed.) (2001), *Handbook of Lasers*, Boca Raton, CRC Press

The following set of conference proceedings are from a series of international conferences held every 2 years since 1990.

G. J. Tallents (Ed.)(1991) , *IOP Conference Series 116 - X-ray Lasers 1990*, , Bristol: IOP Publishing Ltd.

E. E. Fill (Ed.)(1992) , *IOP Conference Series 125 - X-ray Lasers 1992*, , Bristol: IOP Publishing Ltd.

D. C. Eder and D. L. Matthews (Eds.)(1994) , *AIP Conference Proceedings 332 - X-ray Lasers 1994*, New York: American Institute of Physics

S. Svanberg and C-G Wahlström (Eds.)(1996) , *IOP Conference Series 151 - X-ray Lasers 1996*, , Bristol: IOP Publishing Ltd.

Y. Kato, H. Takuma, and H. Daido (Eds.)(1999) , *IOP Conference Series 159 - X-ray Lasers 1998*, Bristol: IOP Publishing Ltd.

G. Jamelot, C. Moller, and A. Klisnick (Eds.)(2001) *X-ray Lasers 2000*, J.Phys. IV(France) **11 (Pr2)**

J. J. Rocca (Ed.)(2002 in press), *AIP Conference Proceedings 641 - X-ray Lasers 2002*, New York: American Institute of Physics

Jie Zhang (Ed.)(2005) , *IOP Conference Series 186 - X-ray Lasers 2004*. Bristol: IOP Publishing Ltd.

P. V. Nickles and K. A. Janulewicz (Eds.)(2007), *Springer Proceedings in Physics Volume 115 - X-ray Lasers 2006.* Dordrecht: Springer

C. L. S. Lewis and D. Riley (Eds.)(2009), *Springer Proceedings in Physics Volume 130 - X-ray Lasers 2008.* Dordrecht: Springer

J. Lee, C. H. Nam, and K. A. Janulewicz (Eds.)(2011), *Springer Proceedings in Physics Volume 136 - X-ray Lasers 2010.* Dordrecht: Springer

S. Sebban, J. Gautier, D. Ros, and P. Zeitoun (Eds.)(2014), *Springer Proceedings in Physics Volume 147 - X-ray Lasers 2012.* Dordrecht: Springer

Figure 1. Schematic of the grazing incidence pumping geometry (GRIP). The line-focused, uncompressed prepulse is incident on the molybdenum target at normal incidence and creates the initial plasma. This is followed by the line focused CPA short pulse that illuminates the target at a grazing incidence angle of 14 degrees. The grazing incidence also produces a travelling wave illumination such that the target preferentially lases in one direction on the Ni-like Mo line at 18.9 nm.

Figure 2. Energy level diagram for lasing on an inner-shell transition in neon. The XFEL at 1.29 nm photoionizes the 1s electron in neutral neon followed by lasing on the 2p → 1s transition at 1.46 nm in singly ionized neon.

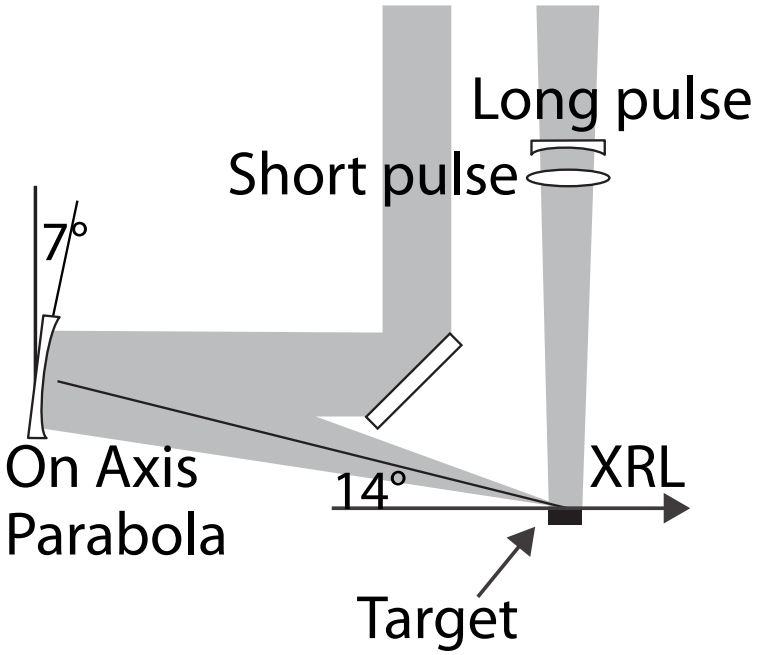

Figure 1. Schematic of the grazing incidence pumping geometry (GRIP). The line-focused, uncompressed prepulse is incident on the molybdenum target at normal incidence and creates the initial plasma. This is followed by the line focused CPA short pulse that illuminates the target at a grazing incidence angle of 14 degrees. The grazing incidence also produces a travelling wave illumination such that the target preferentially lases in one direction on the Ni-like Mo line at 18.9 nm.

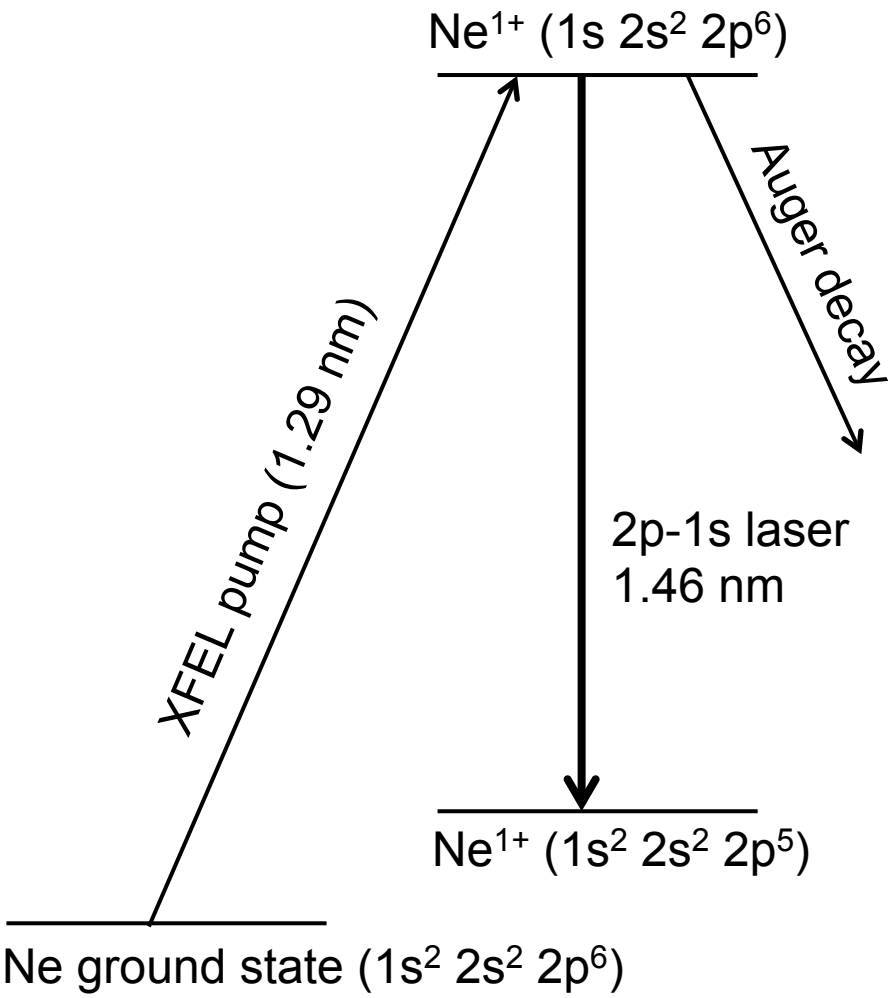

Figure 2. Energy level diagram for lasing on an inner-shell transition in neon. The XFEL at 1.29 nm photoionizes the 1s electron in neutral neon followed by lasing on the 2p → 1s transition at 1.46 nm in singly ionized neon.